

Remote sensing of clouds and water vapor by microwave limb sounding

Dong L Wu

Jet Propulsion Laboratory, California Institute of Technology
4800 Oak Grove Drive, Pasadena, CA 91109, USA

ABSTRACT

Passive radiometers at 100-700 GHz offer great potential for remote sensing of cirrus clouds and upper-tropospheric water vapor from space because radiation at these frequencies can penetrate and interact with cirrus clouds without being cut off at/near cloud surface. This paper focuses mostly on satellite microwave observations from UARS MLS (Upper Atmosphere Research Satellite Microwave Limb Sounder) at 186.5 and 203.2 GHz. Advantages of limb-viewing geometry include better vertical resolution and less contamination of Earth's surface conditions since the limb background radiance depends only on pointing and water vapor abundance. MLS radiance measurements show that water vapor and cloud signals are separable with frequencies of different sensitivities to water vapor. The cloud-induced radiances can be used to directly retrieve ice water content at 14-18km altitudes if the ice particles are smaller than 100 microns. Model simulations at these frequencies are also presented for various cloud types and heights. With the modified MLS radiative transfer model, we are able to simulate limb and nadir radiances at all frequencies between 10 and 1000GHz for both cloudy and clear atmospheres. Our sensitivity studies show that brightness temperature depression at the lowest MLS tangent height can be used to infer cloud height and ice content in the upper troposphere. With more channels near 122, 240, and 640 GHz, we find that the chance of separating cirrus cloud and water vapor is greatly enhanced, and these radiometers are to be flown as the future MLS on board NASA CHEM-1 spacecraft.

Keywords: millimeter and submillimeter-wave, remote sensing, cloud ice content, cloud scattering, cloud emission

1. INTRODUCTION

Cirrus clouds are recognized to play an important role in the Earth's climate and weather systems.¹ However, global observations of cirrus clouds remain limited. For example, ice water content (IWC), an important variable for understanding cloud physical and radiative processes, has not yet been obtained directly from satellite sensors. It is difficult for infrared (IR) and visible techniques because of their poor cloud penetration ability. Nadir viewing microwave sensors (e.g. SSM/I, MSU), operated at various frequencies between 20 and 85 GHz, are able to provide some information on ice water path over ocean but not much on vertical structures of cloud systems and very little on high clouds.²

Remote sensing of cirrus with millimeter and sub-millimeter wave radiometers has been studied intensively by a number of authors,³⁻⁶ showing great potential of this technique for obtaining cloud ice content and particle size information. Most interestingly, cirrus can produce sensible signals in brightness temperature through both scattering and emission. Brightness temperature due to emission is proportional to the total ice mass of cloud as long as particles are much smaller than the wavelength. In the scattering case, upwelling rightness temperature is depressed due to scattering loss in the radiative transfer. The brightness temperature depression can be related to cloud ice mass by assuming some particle size distributions. In either situation one needs to separate between cloud ice and water vapor before retrieving any cloud parameters, and this requires a multi-frequency technique such that these radiances have different sensitivities to water vapor but the relatively same sensitivity to cloud ice.

UARS MLS (Upper Atmosphere Research Satellite Microwave Limb Sounder) has such capability with two radiometers near 183 and 205 GHz to separate cloud and water vapor signals.⁷⁻⁸ The two radiometers have 75 channels that span over 183.1-186.5 GHz and 200.1-206.4 GHz in frequency. Although the instrument is not

designed for tropospheric measurements, it has good sensitivity to upper-tropospheric water vapor and cirrus ice, and the radiances can be used to retrieve these variables when the antenna scans through the troposphere.⁹ Our recent studies show that upper tropospheric water vapor and cloud ice can be simultaneously retrieved from radiances at 186.5 and 203.2-GHz channels, and this paper will describe and discuss technical aspects of the retrieval approach.

2. MLS RADIANCES

During a regular scan, MLS step-scans the atmospheric limb in ~65 seconds at 2 seconds/step from ~90 km to the surface with increments of ~5 km in the mesosphere and 1-3 km in the stratosphere and troposphere. The MLS viewing direction is 90° from the satellite velocity vector. Since UARS moves at a speed of 7.5km/s, each sample is not only separated by a vertical displacement but also by ~15km in the horizontal direction. For the 183 and 205GHz radiometers the vertical width of MLS field-of-view (FOV) is ~3km at the tangent point, a better vertical resolution than most nadir-viewing radiometers.

Figure 1 shows measured 203-GHz radiance profiles under clear and cloudy situations. In a clear and dry atmosphere the limb-scanned radiance increases with decreasing tangent height due to emission from dry-air (continuum and molecular oxygen). Water vapor continuum emission provides additional radiances if the atmosphere is moist, and the difference between the dry-air and moist-air profiles is essentially the sensitivity to water vapor. In the presence of cirrus, the radiance can vary significantly from point to point since each sample is also separated by ~15km in the horizontal direction, which could deal with a completely different cloud cluster. However, one of the advantages of the narrow MLS FOV is to allow the clear separation of high and low level clouds.

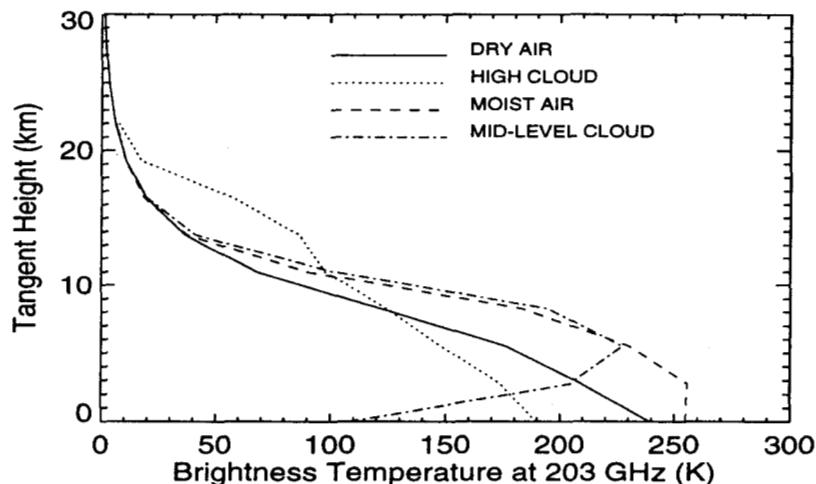


Figure 1. Examples of MLS 203-GHz radiance profiles. A high-latitude wintertime profile is selected for radiance profiles in clear-and-dry air. The profile for moist air is a typical curve observed by MLS in the tropics. The radiance profiles are distorted in a cloudy sky, showing unusually large radiances at 14-20km due to high-cloud emission and the radiance depression below 5km due to scattering expected from large ice particles in mid-level clouds.

In cloudy conditions MLS radiance profiles may be divided into two categories according to the relative importance of scattering and emission processes in the radiative transfer. For higher clouds (14-20km) it is likely to have little scattering because of fewer ice particles greater than 100 μ m (since the wavelengths are much larger than the particles sizes).¹⁰ In other words, at tangent heights above 14km, MLS radiances are determined primarily by emission/absorption processes. For most low clouds, scattering is the dominant process because of the increasing number of large-size ice particles.^{11,4} MLS can observe these low clouds as the antenna points below 5km tangent height.

In the presence of high clouds, the radiance usually shows a larger brightness temperature (T_b) at tangent heights above ~14km, which can be produced by the thermal emission of cloud ice. As shown in Figure 1, sometimes the signal can be 40K above the dry/water vapor continua at ~16km. If there is no scattering in these cases, MLS would

be an excellent technique to measure cloud ice mass since the radiance is only proportional to the ice mass and independent of particle size distributions. Most profiles of this kind are found in the tropical and subtropical regions where deep convection is active.

In the low cloud cases, MLS radiances show a significant reduction in T_b at tangent heights below 5 km. The depression in T_b , sometimes as high as 150K, is caused by scattering of large ice particles in mid-level clouds. It is possible to retrieve ice water path (IWP), or a column ice mass, from the depression T_b but knowledge of particle size distributions is needed.⁴ The retrieval can be more complicated since one must know water vapor profile in order to determine the path length.

3. SEPARATION OF WATER VAPOR AND CLOUD

In the high-cloud case, cloud and water vapor signals can be reasonably separated using radiances of different frequencies. For UARS MLS we use the radiances at 186.5 and 203.2 GHz because of their significantly different sensitivities to water vapor. The 186.5GHz channel is more sensitive to water vapor since it is closer to 183.3GHz water line.

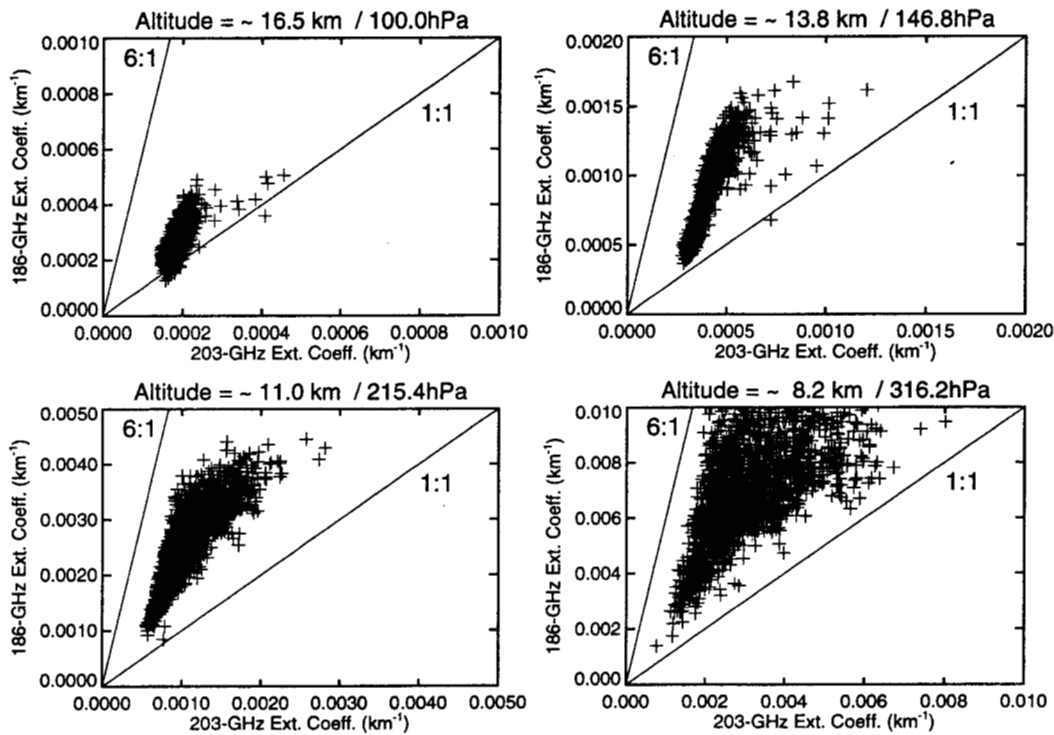


Figure 2. Absorption coefficients at 186.5 and 203.2 GHz frequencies calculated from MLS radiances assuming no scattering.

In the upper troposphere and lower stratosphere, three emission sources are most important at 203 GHz: dry air, water vapor, and ice clouds. In theory the dry air emission can be well determined if tangent pressure and temperature are known since it comes mainly from oxygen lines and collision-induced emissions among major molecules.¹²⁻¹³ However, the modeled dry air continuum is known to about 20% accuracy at 200 GHz, which is not good enough for the water vapor/ice retrievals. Hence, an empirical function for the dry air continuum was derived from MLS data to achieve an accuracy of 5% or better. In addition, emissions from other atmospheric constituents are also need taken into account since the MLS channels were designed to be close to some of the absorption lines of these molecules (i.e., O_3 , HNO_3 , and N_2O). Nevertheless, these contributions are much smaller than those from water vapor, ice, and dry-air continua.

Figure 2 shows the correlation between the absorption coefficients at 186.5 and 203.2 GHz. A good linear relation is found at 16.5 and 13.8 km, showing a slope of 6:1 as expected for water vapor continuum emissions. A few measurements outside the cluster, characterized by lower ratios and larger 203.2-GHz coefficients, are indicative of the presence of ice cloud. These points can be separated using the decision diagram illustrated in Figure 3b. The cloud absorption coefficient is proportional to IWC in the long-wave approximation.¹⁴ From the ice permittivity model,¹⁵ 1K is about $1\text{mg}/\text{m}^3$ at 16km and the detecting threshold for IWC is $\sim 5\text{ mg}/\text{m}^3$. It is important to recognize that the cloud IWC from MLS is an average over a 300 km long, 30 km wide and 3 km high volume.

Poorer correlation at lower tangent heights (11km and 8.2km) is likely due to increasing importance of scattering by large ice particles. At these tangent heights, absorption and scattering processes are equally important, making the radiances difficult to interpret. Therefore, in studying cloud scattering effects we go directly to the radiances at tangent heights below 5km where scattering is the dominant process.

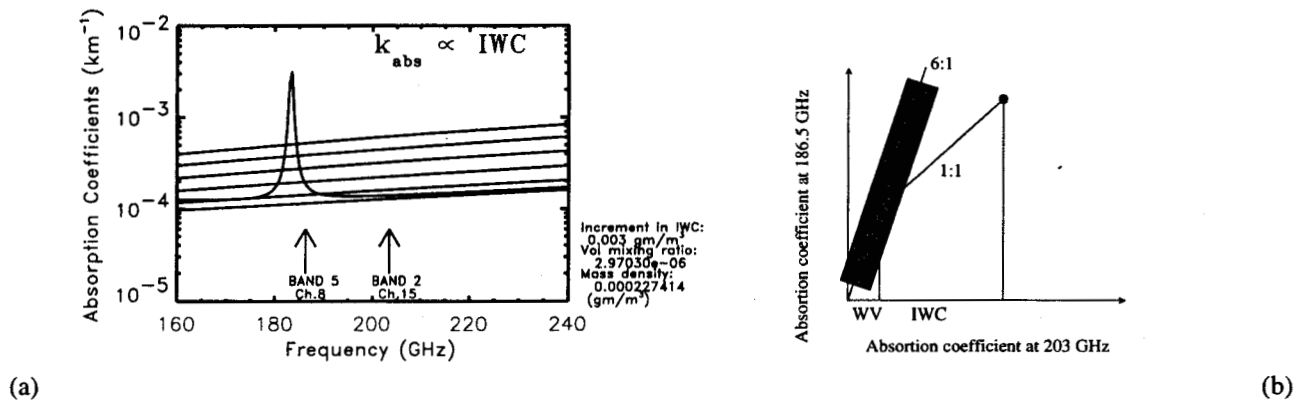


Figure 3. (a) Ice and water vapor absorption at 180-220 GHz frequencies; (b) Decision areas for clouds(1:1) and water vapor(6:1).

4. MLS RADIANCE DEPRESSION DUE TO CLOUD SCATTERING

Figure 4 is an example of MLS 203.2GHz radiances at 5km tangent heights. The depression in T_b is evident at several places of the orbit, producing 20-100K signals as a result of cloud scattering. Since each measurement is separated by $\sim 15\text{km}$ in horizontal distance, a cloud hit may not necessarily relate to the next due to high variability of clouds. This example shows three large cloud clusters near 50°S , 10°S and 10°N , and the strongest depression, as often seen in MLS data, occurred in the tropics. The depression signal is usually more scattered across latitude than the saturated radiance produced by water vapor, reflecting the nature of cloud and water vapor distributions in the upper atmosphere. However, to correctly interpret the T_b depression and retrieve physical cloud parameters, a radiative transfer model is needed.

5. RADIATIVE TRANSFER MODEL

We have built a 32-stream radiative transfer model to simulate MLS radiances in a cloudy atmosphere. The model is able to compute both nadir and limb viewing radiances by incorporating 44 O_2 , 31 H_2O , 93 O^{18}O , and 17 H_2O^{18} lines from the JPL spectral catalog with the Van Vleck-Weisskopf lineshape. For the dry-air continuum, we include the Debye term¹⁶ and contributions from collision-induced-absorption.⁹ For the water vapor continuum, we choose the empirical form put forward by Godon et al.¹⁷ and fit it to MLS and other laboratory measurements.¹⁸⁻²⁰ The model has an option for different surface types (land, ocean, and sea ice) but they turn out to be not important for the frequencies of interest.

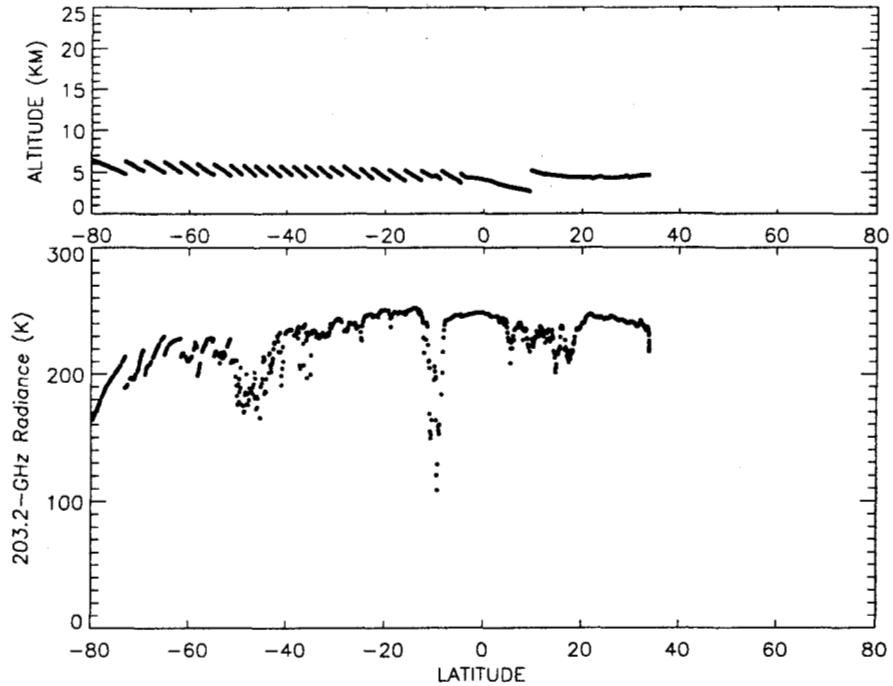


Figure 4. MLS 203.2GHz radiance from the third orbit on 4 April 1996 during a special limb-tracking operation. The limb-tracking is an MLS observing mode in which the instrument views the atmospheric limb at a fixed tangent height continuously during the day. On this day, the tangent height was fixed at 5km, but as shown in the upper panel, the pointing must be adjusted regularly to meet the requirement. The 203.2GHz radiance is mostly saturated at this tangent height in the tropics and subtropics where humidity is high. It is nearly saturated at high latitudes, showing T_b of 200-220K with the discontinuities synchronized to tangent height adjustments. The radiance depressions are those sharply perturbed measurements well below the saturated temperature established by nearby points.

The model is configured to contain 32 scattering angles on a half plane, 80 atmospheric layer (with 0.5km resolution) above the surface, 55 tangent heights between the nadir and 30km (35 above and 20 below the surface). Multiple scattering is not considered at present since it is a second order effect²¹ and all ice particles are assumed as a sphere. For the cloud model, we adopt ice refractive index model by Hufford¹⁵ and allocate 40 size bins between 0 and 5000 microns. To study the sensitivity to the particle size distribution, we parameterize the number distribution in the following form:

$$N(D) = N_0 (10^{-5} + D^{-1.9}) e^{-bD} \quad \text{m}^{-3} \mu\text{m}^{-1}$$

where N_0 is determined by IWC, D is particle diameter in micron, and b is a parameter to adjust the shape of the distribution. The larger b , the fewer large particles. Figure 5 shows four different shapes with the same IWC.

The averaged phase function of cirrus clouds is very important for understanding MLS radiance depression due to ice particle scattering. Based on these phase functions one could simply argue that the most severe T_b depression would produce a radiance equal to about one half of its saturated value. This is because the phase functions are symmetric about the line-of-sight (LOS), producing roughly a half of the radiance scattered from the emissions below the LOS (which are mostly saturated) and the a half scattered from space (which is nearly nothing). The sum is close to one half of its saturated value. This is consistent with MLS observations which show the depressed radiances are rarely below 100K given that the saturated temperature is about 220K in the tropics.

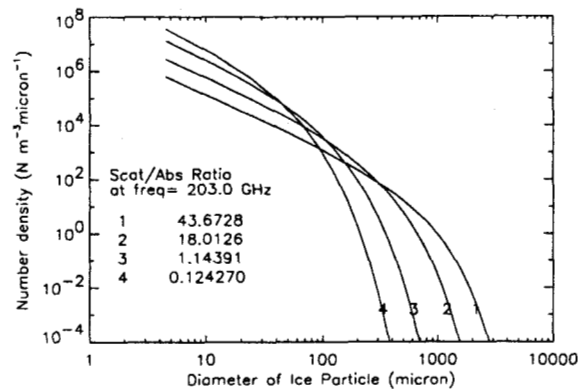


Figure 5. Particle size distributions likely observed in the cirrus at altitudes above 8km. Also listed in the diagram is the total scattering/absorption coefficient ratio, which shows the relative importance of the two processes.

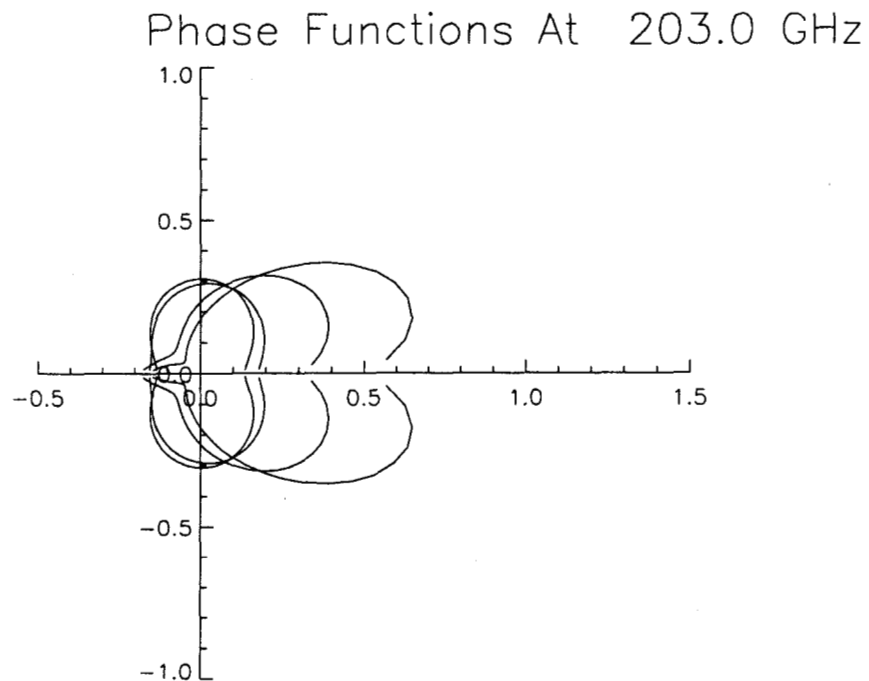


Figure 6. Averaged phase functions for particle size distributions from Figure 5. The horizontal axis is the line-of-sight direction. For the distributions with more large particles, the phase functions become more significantly biased toward the forward scattering. It is interesting to note that the first lobe is not aligned with the line-of-sight.

6. SIMULATED AND MEASURED RADIANCES

Figure 7 shows simulated brightness temperature depressions at 203.2 and 186.5 GHz as a function of cloud height. In these simulations, we insert a 0.5km-thick cloud to the atmosphere and assume 100% saturation below/within the cloud. All other atmospheric conditions are kept as the same except for changing cloud height in each calculation. Since the 203.2-GHz channel is farther from the 183.3-GHz water line, as shown in Figure 7, it can penetrate deeper into the atmosphere to sense clouds at lower altitudes. In this particular case, the 203.2-GHz channel is cutoff around 5km while the 186.5-GHz channel is stopped at ~9km. The cutoff altitude depends not only on frequency but also on water vapor abundance. With less water vapor in the air, these channels can penetrate further into the atmosphere. The depression shows a slight decreasing trend above 10-12km because of the emission contribution as discussed early on.

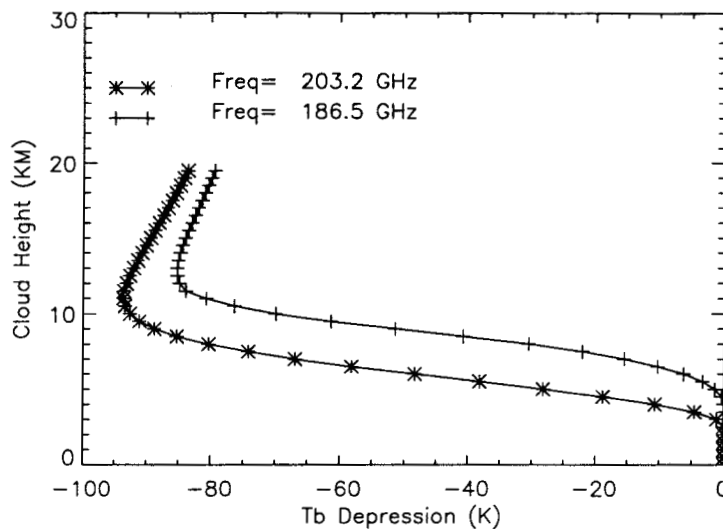


Figure 7. Sensitivity to cloud height. T_b depression is defined as the radiance difference between cloudy and clear atmospheres at the tangent height pointed to the surface.

The height dependence of cloud sensitivity can be also viewed as the contribution function of the scattering signal. Retrieving cloud IWP from T_b depression is limited by the cutoff altitude. However, with several frequencies of different water vapor sensitivity, one may be able to resolve the vertical distribution of cloud ice content. If the frequencies are a few hundred GHz apart, one should also be able to infer particle size information to improve the IWP retrieval.⁴ The future MLS, which will be flown on NASA CHEM-1 spacecraft in 2002, will have 190, 240, 640 GHz radiometers that can be jointly used for retrieving cirrus ice content in the upper atmosphere.²²

To simulate all possible cloud conditions, we generate five categories for IWC in addition to four particle size distributions shown in Figure 5. We place a 4-km cloud layer at 4km as a low cloud and at 12km as a high cloud condition, respectively. Simulated radiances are shown in Figure 8 for UARS MLS frequencies at 203.2 and 186.5 GHz. As expected for different visibility at these frequencies, the high cloud would produce a depression for both channels while the low cloud gives a reduction mostly to the 203.2-GHz channel.

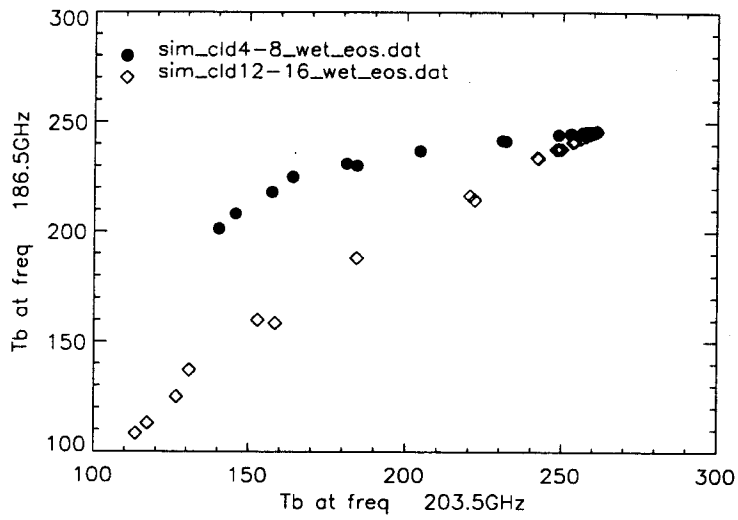


Figure 8. Simulated radiances at 203.2 and 186.5 GHz for cloud base heights at 4km (dots) and 12km (diamonds). The points for each simulation include all cloud categories.

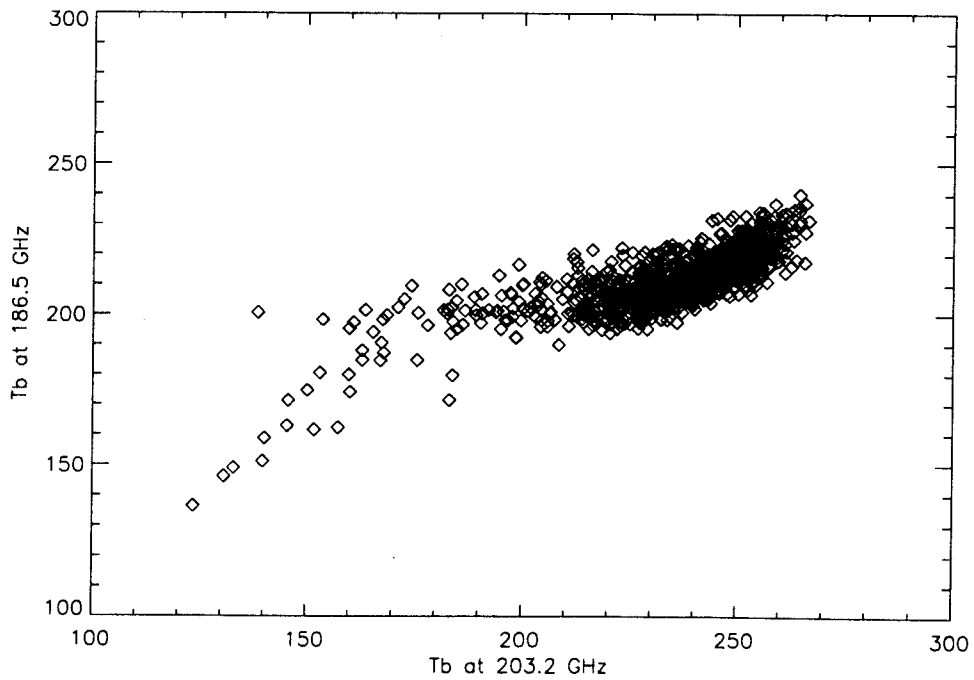


Figure 9. Brightness temperatures at 203.2 and 186.5 GHz as measured by MLS on 27 February 1992. Similar to the simulations, the radiances are from the lowest tangent height within a scan, which is usually below 5km, and they would be mostly saturated due to moist air.

Figure 9 shows MLS radiances at 203.2 and 186.5GHz observed on 27 February 1992. From the simulations in Figure 8, we anticipate that most measurements, with the 203.2GHz radiance greater than 160K and the 186.5GHz radiance greater than 180K, are likely associated with low cloud scattering. There are a few highly depressed measurements, with the 203.2GHz radiance below 160K and the 186.5GHz radiance below 180K, which are likely associated with some high clouds.

7. FUTURE WORK

Effects of cirrus on millimeter and submillimeter-wave radiances need to be investigated further by validating the assumptions used in the analysis and improving the accuracy of radiative transfer models. Specifically, the following areas require more comprehensive studies in the near future:

1. A statistical evaluation is needed for the ice particle size distribution of cirrus clouds above 14km. The assumption made for ice particles greater than 100 micron is critical in MLS ice content measurement, which provides a simple and promising technique to measure ice content in the upper troposphere.
2. For scattering clouds, what are the dependence of T_b depression on cloud height, water vapor distribution, ice content, and particle size distribution? Many sensitivity studies are needed for distinguishing the effects by these highly varying parameters.
3. In order to be accurate in all the simulations required by 2), we need to improve the spectroscopy of dry and water vapor continuum coefficients at frequencies up to 700 GHz. The coefficients used by current models are not very well validated particularly at higher frequencies.
4. UARS MLS radiances need to be further analyzed with better model simulations and cloud classification schemes. In addition to the 203.2 and 186.5GHz radiances, MLS radiances at 183.5GHz could provide more information on cloud height and ice content since it is closer to the 183.3GHz water emission. As discussed in Figure 7, radiance channels with greater optical depth would be cut off at a higher altitude and therefore help the cloud height detection.

8. ACKNOWLEDGMENT

This research was performed at the Jet Propulsion Laboratory, California Institute of Technology, under contract with the U.S. National Aeronautics and Space Administration.

9. REFERENCES

1. Wielicki, B. A., et al., "Mission to Planet Earth: Role of clouds and radiation in climate", *Bull. Amer. Meteor. Soc.*, 76, 2125-2152, 1995.
2. Bauer, P., and P. Schuessel, "Rainfall, total water, ice water, and water vapor over sea from polarized microwave simulations and SSM/I data", *JGR*, 20,737-20,795, 1993.
3. Gasiewski, A. J., "Numerical sensitivity analysis of passive EHF and SMMW channels to tropospheric water vapor, clouds and precipitation", *IEEE Trans. Geosci. Remote Sens.*, 30(5), 859-870, 1992.
4. Evans, K. F., and G. L. Stephens, "Microwave radiative transfer through clouds composed of realistically shaped ice crystals. Part II: Remote sensing of ice clouds". *J. Atmos. Sci.*, 52, 2058-2072, 1995.
5. Evans, K. F., S. J. Walter, A. J. Heymsfield and M. N. Deeter, "Modeling of submillimeter passive remote sensing of cirrus clouds". *J. App. Meteor.*, 37, 184-205, 1997.
6. Wang, J. R., et al., "Observations of cirrus clouds with airborne MIR, CLS, and MAS during SUCCESS". *Geophys. Res. Lett.*, 25, 1145-1148, 1998.
7. Waters, J. W., "Microwave limb sounding. Atmospheric Remote Sensing by Microwave Radiometry". M. A. Janssen, Ed., John Wiley and Sons, Inc., 572 pp., 1993.
8. Barath, F., et al., "The Upper Atmosphere Research Satellite Microwave Limb Sounder instrument", *J. Geophys. Res.*, 98, 10,751-10,762, 1993.
9. Read, W. G., et al., "Upper-tropospheric water vapor from UARS MLS", *Bull. Am. Met. Soc.*, 76, 2381-2389, 1995.
10. Knollenberg, R. G., K. Kelly, and J. C. Wilson, "Measurements of high number densities of ice crystals in the tops of tropical cumulonimbus". *J. Geophys. Res.*, 98, 8639-8664, 1993.

11. Heymsfield, A. J., and C. M. R. Platt, "A parameterization of the particle size spectrum of ice clouds in terms of the ambient temperature and the ice water content". *J. Atmos. Sci.*, 41, 846-855, 1984.
12. Borysow, A., and L. Frommhold, "Collision-induced rotranslational absorption spectra of N₂-N₂ pairs for temperatures from 50 to 300 K". *Astrophys. J.*, 311, 1043-1057, 1986.
13. Dagg, I. R., A. Anderson, S. Yan, W. Smith, and L. A. A. Read, "Collision-induced absorption in nitrogen at low temperatures". *Can. J. Phys.*, 63, 625-631, 1985.
14. Gunn, K. L. S., and T. W. R. East, "The microwave properties of precipitation particles". *Quart. J. Roy. Meteor. Soc.*, 80, 522-545, 1954.
15. Hufford, G., "A mode for the complex permittivity of ice at frequencies below 1 THz". *Int. J. Infrared Millimeter Waves*, 12, 677-682, 1991.
16. Liebe, H. J., "MAM-An atmospheric millimeter-wave propagation model". *International J. of Infrared. Millimeter Waves*, 10, 631-650, 1989.
17. Godon, M, J. Carlier, and A. Bauer, "Laboratory studies of water vapor absorption in the atmospheric window at 213GHz". *J. Quant. Spectrosc. Radiat. Transfer*, 47, 275-285, 1992.
18. Bauer, A. and M. Godon, "Temperature dependence of water-vapor absorption in linewings at 190GHz". *J. Quant. Spectrosc. Radiat. Transfer*, 46, 211-220, 1991.
19. Bauer, A., M. Godon, J. Carlier, Q. Ma, and R. H. Tipping, "Absorption by H₂O and H₂O-N₂ mixtures at 153GHz". *J. Quant. Spectrosc. Radiat. Transfer*, 50, 463-475, 1993.
20. Buaer, A., M. Godon, J. Carlier, and Q. Ma, "Water vapor absorption in the atmospheric window at 239GHz". *J. Quant. Spectrosc. Radiat. Transfer*, 53, 411-423, 1995.
21. Bond, S. T., "The potential effect of cirrus on Microwave Limb Sounder retrievals". Ph.D. Dissertation, Univ. of Edinburgh, UK, 1996.
22. Waters, J. W., et al., "The UARS and EOS Microwave Limb Sounder (MLS) Experiments", *J. Atmos. Sci.*, in press, 1998.